Fuel 117 (2014) 1085–1092

Contents lists available at ScienceDirect

Fuel

journal homepage: www.elsevier.com/locate/fuel

Effects of pelletization conditions on breaking strength and dimensional stability of Douglas fir pellet

Pak Yiu Lam [a], Pak Sui Lam [a,*], Shahab Sokhansanj [a,b], Xiaotao T. Bi [a], C. Jim Lim [a], Staffan Melin [a]

[a] *Department of Chemical and Biological Engineering, University of British Columbia, 2360 East Mall, Vancouver, BC V6T 1Z3, Canada*
[b] *Environmental Science Division, Oak Ridge National Laboratory, P.O. Box 2008, Oak Ridge, TN 37831-6422, United States*

HIGHLIGHTS

- The compression behaviour of Douglas fir particles was investigated.
- Temperature, pressure and stress relaxation were significant to the pellet's mechanical properties.
- Walker, Jones, Kawakita and Ludde were the best compaction models for Douglas fir.
- The best pelletizing conditions for Douglas fir with a particle size of 1.19 mm was 100 °C, 126 MPa and 30 s relaxation time.

ARTICLE INFO

Article history:
Received 18 July 2013
Received in revised form 28 September 2013
Accepted 14 October 2013
Available online 26 October 2013

Keywords:
Wood pellets
Elastic modulus
Stress relaxation
Hardness
Pelletization

ABSTRACT

The compression behavior of Douglas fir ground particles using a heated piston–cylinder unit was investigated. A complete randomized design (CRD) of experiment with three factors (die temperature, applied pressure and relaxation time), three levels and five replicates were studied. From the analysis of variance (ANOVA) with $\alpha = 0.05$, all of the three pelletization factors were significant parameters to the maximum breaking strength and the relaxed pellet density. The significant factors to the initial pellet density of pellets were the die temperature and the applied pressure. Three out of five compaction models of Walker, Jones, Kawakita and Ludde were well described to the compression behavior of Douglas fir ground particles with R^2 values between 0.90 and 0.99. The optimum processing condition to produce the best quality of Douglas fir pellets was 100 °C die temperature, 126 MPa applied pressure and 30 s relaxation time.

© 2013 Elsevier Ltd. All rights reserved.

1. Introduction

Douglas fir (*Pseudotsuga menziesii*, L.) is one of the many abundant species of coniferous softwood in the western coast of North America. It is widely used for structural timber, lumber, and furniture; meanwhile, the wood processing generates substantial amounts of residual by-products such as sawdust and shavings. The recovered Douglas fir sawdust and shavings are good candidates for producing fuel pellets for energy production, in replacement of coal. Douglas fir ground particles with a mean particle size of 1–2 mm can be pelletized into Douglas fir pellets with a 6–8 mm diameter and 12–25 mm length [1,2]. It was found that the wood pellets longer than 13 mm decreased the average burning temperature of a pellet stove by 31% and the flue gas temperature by 25% [3]. Because of this, Douglas fir pellets with a shorter length are preferred for efficient combustion.

Douglas fir pellets are required to be handled and stored safely in order to minimize risks for health and safety. The biodegradation of the wood pellets diminishes the mechanical properties and will contribute to mass loss during storage and transportation [4]. Consequently, the major limitation of using Douglas fir pellets as fuel is low durability. Durability is defined as the weight percentage of the remaining unbroken wood pellets to the total sample size of the wood pellets after tumbling, according to the European standard EN 15210-1 [5]. The durability of wood pellets is well correlated with the hardness values measured from the material properties testers [6]. In essence, the durability of Douglas fir pellets is highly dependent on the compression behavior of the ground particles.

Extensive research has evaluated the pelletization mechanisms of Douglas fir ground particles with or without pre-treatments [7–9]. The compression behavior of biomass ground particles were studied in different models [8,10–13]. Jones [14], Heckel [15], Cooper and Eaton [16], Kawakita and Ludde [17] and Panelli and Filho [18] models were studied to determine the pressure–volume and the pressure–density relationship of barley, canola, oat and wheat

---

* Corresponding author. Tel.: +1 6043558811.
E-mail addresses: wilsonlam82@yahoo.com, wilsonlam007@gmail.com (P.S. Lam).

0016-2361/$ - see front matter © 2013 Elsevier Ltd. All rights reserved.
http://dx.doi.org/10.1016/j.fuel.2013.10.033

straw. Mani et al. reported that the Heckel and Cooper–Eaton model are the most applicable compaction models to describe the compression mechanism of cellulosic agricultural materials [19]. The Kawakita–Ludde model was proposed to describe the compression behavior of soft and fluffy materials [17] and works best only for a limited species of agricultural biomass (barley, canola, oat and wheat). Adapa et al. [10] and Tabil and Sokhansanj [20] reported that the Cooper–Eaton, Heckel and Panelli–Filho models were best fitted with the compression data of alfalfa. Walker's model was used to describe the compression behavior of nonmetallic powders [11,21,22]. There is limited research studying Walker's model on woody and agricultural biomass. Adapa et al. [10] attempted to use the Walker model to describe the compression behavior of fractionated alfalfa. However, a good fit was not obtained compared to other compaction models. Comoglu [22] reported that the two most commonly used compaction models; Heckel [15] and Kawakita and Ludde [17], failed to relate the densification behavior of wood to their physical and mechanical properties.

The objective of this research is to study the effect of pelletization conditions (die temperature, applied pressure and stress relaxation) on the pellet's mechanical strength and dimensional stability. A complete randomized design (CRD) of experiment with three factors, three levels, and five replicates is introduced. In addition, this research evaluates the fittings of different compaction models for Douglas fir pellets. The experimental results could be further applied to study the continuous pelletizing process with an automated control system.

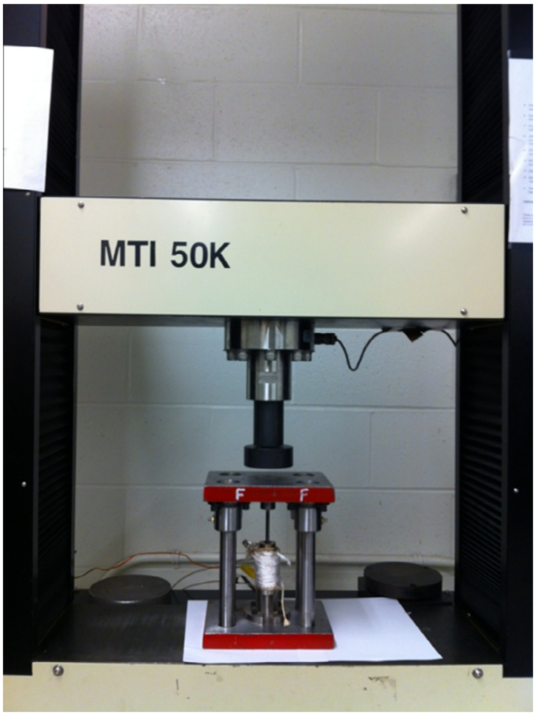

Fig. 1. Experimental setup with a MTI system and the die to produce pellets.

2. Materials and methods

2.1. Materials

As-received Douglas fir (*Pseudotsuga menziesii* L.) with 55% (w.b.) moisture content were obtained from piles of wood chips at the Fibreco facilities in North Vancouver, B.C., Canada. The woodchips were ground into powder using a laboratory knife mill equipped with a 6 mm screen size. The particle size analysis was performed according to the ASABE S319.3 standard [23]. The mean particle size of the powder was 1.19 mm. The recovered powders from the knife mill were conditioned to 11.3% (w.b.) moisture content prior to pelletization.

2.2. Pelletization

A removable fixture and a single die pelletizing unit (MTI 50 K, Measurement Technology Inc., Atlanta, USA) was used to produce wood pellets (Fig. 1). The fixture composed of a top part and a bottom part. The top part with a 6.35 mm diameter iron rod connecting to the top flange was controlled by the crosshead of the MTI machine. The bottom part was installed with four bars at the corners to provide an accurate alignment between the rod and the die channel during vertical movement. The channel of the die is 70 mm long and 6.35 mm in diameter. The die was pre-heated by a heating tape connected to a controller. The heat supply mimics the heat generated by the friction during pelletization in the industrial pellet mill. It also ensures a uniform temperature gradient over the die. For each experimental trial, approximately 0.85 g of Douglas fir powder was fed into the die channel and compressed at 10 mm/min. The compression force and displacement data were recorded by the computer data logging system connecting to the pelletizing unit. The total energy required to produce a pellet is the total area under the force versus displacement curve. In order to study the effect of process conditions on pellet quality, a complete randomized design (CRD) of experiment with three factors, three levels, and five replicates is introduced (Table 1). Five pellets were made for each mechanical condition.

2.3. Stress relaxation and hardness test

The effect of the stress relaxation behavior of thermally treated Douglas fir pellets on its dimensional stability was investigated [8]. This was done by measuring the rate of decrease of residual stress in 30 s and the associated data were normalized, linearized and represented as a straight line:

$$\frac{\sigma_0 t}{\sigma_0 - \sigma(t)} = k_1 + k_2 t \tag{1}$$

where σ_0 is the initial stress, GPa, $\sigma(t)$ the stress after time t at relaxation, GPa, t is time, s and k_1 and k_2 are constants.

The viscoelastic slope, k_2, can be used to quantify the degree of plastic flow under compaction [24]. Materials with a high visco–elastic slope value, k_2, exhibit a greater degree of plastic flow under compression. This parameter was found to correlate well with forming strong pellets. For example, materials that displayed large viscoelastic slope constants formed strong tablets at low compaction temperatures [24]. The slope k_2 of the straight line must be greater than one, and from a rheological point of view, the slope can be considered as an index of how solid the compacted specimen is on a short time scale. Any large value of greater than one is an indication of the existence of stresses that will

Table 1
Design of experiment of pelletization.

Parameters[a]	Units	Low (−1)	Normal (0)	High (+1)
Die temperature	°C	70	100	130
Applied pressure	MPa	63	126	190
Relaxation time	s	5	15	30

[a] Number of measurements, $N = 5$.

Table 2
Dimension and density of Douglas fir pellet with respect to different pelletization conditions.

Die temperature (°C)	Pressure (MPa)	Relaxation time (s)	Mass[a] (g)		Length[a] (mm)		Diameter[a] (mm)		True density[b] (g/cm³)		Pellet density[b] (g/cm³)		Reduction of particle density (%)
			Average	SD	Average	SD	Average	SD	Average	SD	Average	SD	
Measured after die removal													
70	63	5	0.80	0.03	25.8	0.9	6.5	0.0	1.36	0.00	0.93	0.01	–
		15	0.81	0.01	26.1	0.1	6.5	0.0	1.33	0.00	0.94	0.01	–
		30	0.82	0.02	26.2	0.7	6.5	0.1	1.35	0.00	0.95	0.02	–
	126	5	0.84	0.01	22.6	0.2	6.4	0.0	1.30	0.00	1.14	0.03	–
		15	0.84	0.01	22.5	0.3	6.5	0.0	1.30	0.00	1.11	0.02	–
		30	0.83	0.01	22.5	0.2	6.5	0.0	1.31	0.00	1.11	0.02	–
	190	5	0.82	0.01	21.2	0.5	6.5	0.0	1.28	0.01	1.16	0.01	–
		15	0.84	0.01	21.6	0.4	6.5	0.0	1.27	0.00	1.16	0.02	–
		30	0.84	0.00	21.4	0.4	6.5	0.0	1.29	0.00	1.16	0.02	–
100	63	5	0.82	0.01	24.7	0.2	6.5	0.0	1.31	0.00	1.00	0.01	–
		15	0.81	0.01	24.1	0.7	6.5	0.0	1.32	0.00	1.03	0.03	–
		30	0.82	0.01	24.2	0.5	6.5	0.0	1.32	0.00	1.02	0.02	–
	126	5	0.83	0.00	21.8	0.6	6.5	0.0	1.29	0.00	1.15	0.03	–
		15	0.83	0.01	21.6	0.2	6.5	0.0	1.30	0.00	1.16	0.01	–
		30	0.82	0.01	21.4	0.7	6.5	0.0	1.30	0.00	1.17	0.03	–
	190	5	0.80	0.04	20.3	0.8	6.5	0.0	1.33	0.00	1.20	0.03	–
		15	0.83	0.01	20.4	0.3	6.5	0.0	1.29	0.00	1.22	0.01	–
		30	0.83	0.00	20.3	0.3	6.5	0.0	1.30	0.00	1.23	0.02	–
130	63	5	0.78	0.00	24.8	0.5	6.5	0.0	1.34	0.00	0.95	0.02	–
		15	0.79	0.01	25.0	0.4	6.5	0.0	1.34	0.00	0.95	0.02	–
		30	0.79	0.00	24.5	0.2	6.5	0.0	1.36	0.00	0.97	0.01	–
	126	5	0.79	0.00	21.0	0.3	6.5	0.0	1.37	0.00	1.13	0.02	–
		15	0.79	0.01	21.1	0.3	6.5	0.0	1.37	0.01	1.12	0.02	–
		30	0.79	0.01	21.1	0.5	6.5	0.0	1.36	0.00	1.13	0.02	–
	190	5	0.78	0.00	19.6	0.3	6.5	0.0	1.38	0.00	1.20	0.02	–
		15	0.79	0.00	20.0	0.2	6.5	0.0	1.37	0.00	1.19	0.01	–
		30	0.79	0.01	19.8	0.4	6.5	0.0	1.37	0.00	1.20	0.03	–
Measured after one week													
70	63	5	0.78	0.03	26.0	0.9	6.5	0.0	–	–	0.90	0.01	2.9
		15	0.81	0.01	26.7	0.5	6.5	0.0	–	–	0.91	0.01	3.1
		30	0.80	0.01	25.8	0.9	6.5	0.0	–	–	0.93	0.04	1.9
	126	5	0.83	0.01	22.8	0.2	6.5	0.0	–	–	1.09	0.02	4.6
		15	0.83	0.01	22.6	0.2	6.5	0.0	–	–	1.09	0.01	1.7
		30	0.83	0.01	22.6	0.3	6.5	0.0	–	–	1.09	0.01	1.1
	190	5	0.82	0.01	21.4	0.6	6.5	0.0	–	–	1.14	0.02	1.4
		15	0.84	0.01	21.8	0.3	6.5	0.0	–	–	1.15	0.02	1.0
		30	0.83	0.01	21.6	0.4	6.5	0.0	–	–	1.15	0.03	1.2
100	63	5	0.81	0.01	24.7	0.6	6.5	0.0	–	–	0.99	0.02	1.2
		15	0.81	0.01	24.3	0.7	6.5	0.0	–	–	0.99	0.03	3.0
		30	0.81	0.01	24.3	0.5	6.5	0.0	–	–	1.00	0.02	1.5
	126	5	0.83	0.00	21.9	0.7	6.5	0.0	–	–	1.14	0.04	1.0
		15	0.83	0.01	21.7	0.2	6.5	0.0	–	–	1.14	0.02	1.2
		30	0.82	0.01	21.5	0.2	6.5	0.0	–	–	1.15	0.02	1.5
	190	5	0.80	0.04	20.4	0.9	6.5	0.0	–	–	1.18	0.01	1.7
		15	0.83	0.01	20.6	0.4	6.5	0.0	–	–	1.20	0.01	1.5
		30	0.83	0.00	20.6	0.2	6.5	0.0	–	–	1.20	0.01	2.0
130	63	5	0.78	0.00	25.0	0.4	6.5	0.0	–	–	0.94	0.02	0.8
		15	0.79	0.01	25.2	0.5	6.5	0.0	–	–	0.94	0.01	1.5
		30	0.79	0.00	24.7	0.3	6.5	0.0	–	–	0.95	0.01	2.1
	126	5	0.79	0.00	21.4	0.2	6.5	0.0	–	–	1.11	0.01	2.4
		15	0.79	0.00	21.7	0.2	6.5	0.0	–	–	1.09	0.01	3.3
		30	0.80	0.01	21.7	0.7	6.5	0.0	–	–	1.10	0.03	2.7
	190	5	0.79	0.00	20.2	0.4	6.5	0.0	–	–	1.17	0.02	2.8
		15	0.79	0.00	20.4	0.1	6.5	0.0	–	–	1.16	0.01	1.9
		30	0.79	0.01	20.3	0.2	6.5	0.0	–	–	1.17	0.02	2.7

[a] Number of measurements, $N = 15$.

[b] Number of measurements, $N = 5$.

eventually remain unrelaxed [25]. The residual stress can also be defined as the percentage of the stress at relaxation time t over the initial stress, %.

Moreyra and Peleg [25] and Scoville and Peleg [26] stated that the asymptotic modulus (E_A) can be an empirical index of solidity, which is the ability of the compressed powder to sustain unrelaxed stresses; E_A is defined as:

$$E_A = \frac{\sigma_0}{\varepsilon}\left(1 - \frac{1}{k_2}\right) \tag{2}$$

where E_A is the asymptotic modulus, GPa, and ε is the strain, dimensionless or m/m.

Eq. (1) can be fitted to the stress relaxation data to estimate k_1 and k_2. The estimated k_2 value is then used in Eq. (2) to calculate E_A.

Table 3
Analysis of variance (ANOVA) of pellet's density and maximum breaking strength with respect to die temperature, compression pressure and relaxation time.

Responses	Maximum breaking strength (MPa)		Initial pellet density (kg/m^3)		Relaxed pellet density (kg/m^3)	
Model components	7					
Number of observations	3 factors × 3 levels × 5 replicates = 135					
	F-value	Prob.	*F*-value	Prob.	*F*-value	Prob.
Relaxation time, s (t)	1.43	0.2450	2.27	0.1084	3.43	0.0361
Die temperature, °C (T)	43.26	<.0001	100.33	<.0001	103.39	<.0001
Compression pressure, MPa (P)	108.14	<.0001	1615.79	<.0001	1391.15	<.0001
$t \times T$	2.74	0.0326	2.66	0.0367	1.00	0.4094
$t \times P$	0.52	0.7204	2.48	0.0481	1.12	0.3486
$T \times P$	1.00	0.4100	5.93	0.0002	4.19	0.0034
$t \times T \times P$	0.32	0.9570	1.00	0.4433	0.41	0.9131

The detailed mathematical proof can be found in the appendix of our previous work [8].

For hardness test, a single pellet was placed on a compression plate fixture of the MTI machine and the 6.35 mm diameter compression rod was set to indent downward at the middle of the pellet. The compression rod was initially moved down until it was barely in contact with the pellet without applying a pre-loading force. The downward loading force was then applied for indentation and the mechanical strength of the pellet was estimated from the maximal point of the force displacement diagram. The maximum breaking strength of a pellet was estimated by the maximum force, *N*, divided by the cross sectional area of the compression rod, mm.

2.4. Physical characterization

The mass, length, and diameter of each pellet were measured immediately after its removal from the cylinder to calculate the initial pellet density. These measurements were repeated after a week's storage. A true density was determined by measuring the total pore volume of a pellet by compressing the nitrogen at 103 kPa into the void spaces of the pellets using a Quantachrome Multipycnometer (Quantachrome, Boyton Beach, FL, USA). The mass of the pellet was measured to 0.01 g precision using an electronic balance (Acculab ALC-80.4, Edgewood, NY).

Moisture content of the ground particles and the pellets were analyzed according to ASABE S358.2 standard [27]. Approximately 1 g of either ground particles or a single pellet was used for moisture content measurement. Triplicate samples were oven dried at 103 °C for 24 h. The ash content of three replicates was determined as the percentage of residue remaining after dry oxidation according to the NREL protocol (NREL/TP-510-42622) (oxidation at 550–600 °C) [28]. The high heating values of the pellets were determined by the oxygen bomb calorimeter (Parr 6100) from two replicates. Elemental analysis was performed on measuring the percentage of carbon (C), hydrogen (H) and oxygen (O) of the samples by an elemental analyzer (Carlo Erba, EA 1108, Italy).

Table 4
Fitted parameters of different compaction models.

Model	Temperature (°C)	Relaxation time (s)	Constants			
			m	*B*	R^2	*SSE*
Walker	–	–	−0.00091	0.005061	0.9585	2.02E−07
	–	5	−0.00092	0.005146	0.9528	7.99E−08
	–	15	−0.00090	0.005008	0.9641	5.61E−08
	–	30	−0.00090	0.005027	0.9600	6.48E−08
	70	–	−0.00099	0.005498	0.9634	7.13E−08
	100	–	−0.00083	0.004636	0.9698	4.00E−08
	130	–	−0.00090	0.005037	0.9730	4.25E−08
			M	*B*	R^2	*SSE*
Jones	–	–	0.1887	6.098	0.9039	2.15E−02
	–	5	0.1980	6.051	0.9126	7.09E−03
	–	15	0.1876	6.102	0.8945	7.76E−03
	–	30	0.1807	6.142	0.9124	6.00E−03
	70	–	0.1964	6.038	0.9386	4.80E−03
	100	–	0.1662	6.233	0.9708	1.57E−03
	130	–	0.2025	6.029	0.9797	1.60E−03
			A	1/*b*	R^2	*SSE*
Kawakita and Ludde model	–		0.6771	26.459	0.9882	2.02E+03
	–	5	0.7027	31.750	0.9894	5.57E+02
	–	15	0.6527	21.573	0.9909	5.47E+02
	–	30	0.6775	26.375	0.9871	7.40E+02
	70	–	0.7210	33.540	0.9958	2.07E+02
	100	–	0.6974	31.604	0.9901	5.33E+02
	130	–	0.6207	15.649	0.9957	2.86E+02
			A	*B*	R^2	*SSE*
Panelli–Filho model	–	–	0.1812	−0.1295	0.7925	1.38E+00
	–	5	0.1650	0.0119	0.8251	3.08E−01
	–	15	0.1901	−0.2149	0.7865	5.18E−01
	–	30	0.1885	−0.1856	0.7904	5.10E−01
	70	–	0.1972	−0.3489	0.9667	7.19E−02
	100	–	0.2063	−0.1679	0.9004	2.52E−01
	130	–	0.1384	0.1460	0.9905	9.78E−03

3. Compaction models

3.1. Walker model

Walker studied the compressibility of powders and developed a model to understand the pressure–volume relationships of calcium carbonate and tetronitromethylamiline [29]. The Walker model was subsequently applied to describe the compaction behavior of biological materials [30]. Walker expressed the volume ratio, V_R, as a function of applied pressure, P, as shown below in Eq. (3).

$$V_R = m \ln P + b \tag{3}$$

where

$$V_R = \frac{V}{V_S} \tag{4}$$

P = applied pressure, MPa; V_R = volume ratio, dimensionless; V = volume of compact at pressure P, m^3; V_S = void free solid material volume, m^3.

3.2. Jones model

Jones [14] expressed the density–pressure data of compacted metal powder in the form of Eq. (5):

$$ln\rho = m \ln P + b \tag{5}$$

where ρ is the bulk density of a compact powder mixture, kg/m^3; m and b are constants, dimensionless. The constants m and b are determined from the intercept and slope of the extrapolated linear region of the plot of $\ln(\rho)$ vs $\ln(P)$. The constant m was equal to the reciprocal of the mean yield pressure required to induce plastic deformation [31]. A material with a large m value (low yield pressure) indicates that the onset of plastic deformation took place at a relatively low pressure and the resulting compressed material is highly compressible.

3.3. Cooper–Eaton model

Cooper–Eaton studied the compression behavior of four ceramic powders [16]. In each case, they assumed that compression was attained by two nearly independent probabilistic processes: the filling of voids having equal size as particles and the filling of voids smaller than the particles. Based on these assumptions, the following Eq. (6) was given:

$$\frac{V_0 - V}{V_0 - V_S} = a_1 e^{-\frac{k_1}{P}} + a_2 e^{-\frac{k_2}{P}} \tag{6}$$

where V_0 = volume of compact at zero pressure, m^3; a_1, a_2, k_1, and k_2 = Cooper-Eaton model constants, dimensionless.

The difficulty in practical use of the equation is the assignment of some physical significance to the constant parameters of this equation. In addition, another drawback of this model is its applicability to only one-component system [22].

3.4. Kawakita and Ludde model

Kawakita and Ludde [17] proposed a compaction model of powders based on the observed relationship between the pressure and the volume by Eq. (7):

$$\frac{P}{C} = \frac{1}{ab} + \frac{P}{a} \tag{7}$$

where,

$$C = \frac{V_0 - V}{V_0} \tag{8}$$

C = degree of volume reduction or engineering strain, dimensionless; a and b = Kawakita–Ludde model constants related to characteristic of the powder, dimensionless.

The Kawakita–Ludde model constants were evaluated from the linear graph of P/C and P. The Kawakita–Ludde model was highly applicable to describe the compression behavior of the soft and fluffy powders [11,17], however particular attention must be paid on the measurement of the initial volume of the powder which will cause large deviation values of V_0. The constant a is equal to the values of $C = C_\infty$ at infinitely large pressure P.

$$C_\infty = \frac{V_0 - V_\infty}{V_0} \tag{9}$$

where V_∞ = net volume of the powder, m^3.

It was reported that the constant a is equal to the initial porosity of the sample, while constant $1/b$ is related to the failure stress in the case of piston compression [19].

3.5. Panelli–Filho model

Panelli–Filho proposed a compaction model based on a new phenomenon [18], Eq. (10):

$$ln \frac{1}{1 - \rho_r} = A\sqrt{P} + B \tag{10}$$

where ρ_r is the relative density of the compact, dimensionless; A is a parameter related to densification of the compact by particle deformation, dimensionless; P is the applied pressure, MPa and B is a parameter related to powder density at the start of compression, dimensionless.

3.6. Statistical analysis

Statistical analysis of variance (ANOVA) was performed using SAS 9.1.3 (SAS Institute Inc., Cary, NC). Multi-linear regression (MLR) was used to model responses of three components: initial pellet density, relaxed pellet density and maximum breaking strength. MLR-models were created from range-scaled factors of pelletization conditions: die temperature, applied pressure and relaxation time. By using the range-scaled factors, differences in magnitude in factors were extinguished when values were recalculated to range from -1 to +1. Thus, the sign of modeled coefficients showed if factors were negatively or positively correlated to the response. The magnitude of the modeled coefficients was equivalent to the impact that each factor had on the response. The MLR models were studied in the following ranges: a die temperature of 70–130 °C, applied pressure of 63–190 MPa, and relaxation time of 5–30 s:

$$y_i = \beta_0 + \beta_1 x_{i1} + \beta_2 x_{i2} + \cdots + \beta_p x_{ip} + \varepsilon_i \quad for\ i = 1, 2, \ldots, n. \tag{11}$$

where y_i is the measured responses, β_i is the estimated parameters of the population regression line, x_i, p represents independent variable of the ith measurement, ε_i is the model deviation.

4. Results and discussion

4.1. Pellet properties

The produced pellets in this study were with 11.3% moisture content (wet basis), 20.2 MJ/kg high heating value (dry basis), 0.18% ash content (mass fraction), 1.42% extractives (mass fraction), lignin content of 30.09% (mass fraction) and with the elemental composition of 48.44% carbon, 6.23% hydrogen, and 45.33% nitrogen (mass fraction). Table 2 lists the physical dimensions and the densities of Douglas fir pellets at different pelletization conditions. At die temperatures 70 and 100 °C, the mass of the pellets ranged between 0.80 and 0.84 g. At die temperature 130 °C, only a slight discrepancy of mass was observed between 0.78 and 0.79 g and this was due to the evaporation of moisture. The pellet length decreased from 26.2 to 19.6 mm with increasing applied pressure, regardless of the other associated factors: die temperature and relaxation time. The true density of pellets decreased from 1.36 to 1.27 g/cm^3 with increasing the applied pressure at a die temperature of 70 °C while the true density of pellets increased from 1.29 to 1.37 g/cm^3 with increasing the applied pressure at a die temperature of 100 and 130 °C. It is observed that the evaporation of moisture caused the shrinkage of the micropores of the micro-fibrils at die temperature 100 and 130 °C, thereby achieving higher true densities. The pellet densities increased from 0.93 to 1.23 g/cm^3 with increasing applied pressure from 63 to 190 MPa. At a die temperature of 100 °C, the pellet densities were higher than that of pellets made with the other die temperatures and corresponding pressure. This was due to the free water of the Douglas fir (i.e. moisture) being vaporized at 100 °C and easily diffused into the middle lamella to activate the lignin as a natural binder for increasing the binding ability of the pellet [32]. It was observed that there was an expansion in pellet length after one week of production. There was no expansion in radial dimension. As a result, the pellet density decreased from 4.6% to 0.8% (Table 2). This information would be an important finding for an industrial design of a silo for pellet storage.

From the results of analysis of variance (ANOVA) of the initial and relaxed pellet density of the pellets (Table 3), it was found that the two factors, die temperature (T), and compression pressure (P), and its interaction ($T \times P$) were the most significant to the initial density of the pellets with $\alpha = 0.05$. The effect of relaxation time (t) was not significant to the initial pellet density but was highly correlated to the relaxed pellet density. This indicated that the relaxation time (t) was an important factor for producing pellets with good dimensional stability. Two multi-linear model equations with their significant production parameters for Douglas fir pellets described the initial pellet density (ρ_1) and the relaxed density (ρ_2) as the following:

$$\rho_1 = 873.187 + 0.0865T + 1.4617P + 0.0021T \times P \tag{12}$$

with $RMSEP = 40.7082$ F-value = 220.03, $R^2 = 0.8344$

$$\rho_2 = 806.773 + 0.4243t + 0.4860T + 1.7862P - 0.0013T \times P \tag{13}$$

with $RMSEP = 40.7082$ F-value = 220.03, $R^2 = 0.8327$

where t is the relaxation time, s, T is the die temperature, °C and P is the die pressure, MPa.

4.2. Compaction models

Table 4 lists the Walker, Jones, Kawawkita and Ludde and Panelli–Filho model at different temperature and relaxation time. The parameters in the first row of different models were fitted by using all of the experimental data points. The parameters from the second to the fourth rows of different models were fitted only with the relaxation time. The parameters from the fifth to the seventh rows of different models were fitted only with the die temperature. Note that the applied pressure was the only independent input of these models in the previous studies [10,19]. The temperature and relaxation time were not included. The Walker model was able to predict the pellet densities at different applied pressure, temperature and relaxation time with R^2 values ranging from 0.95 to 0.97. Thus, the Walker model is independent of temperature and relaxation time. The Jones model showed a higher tendency in predicting the pellet densities in temperature with R^2 values ranging from 0.94 to 0.98, compared to lower R^2 values of relaxation time ranging from 0.90 to 0.91. The Kawakita and Luddel model is highly capable of predicting the initial porosity (a) and the failure stress ($1/b$) with R^2 values ranging from 0.98 to 0.99 regardless of temperature and relaxation time. Since the high die temperature caused the evaporation of material inside the die channel, the initial porosity and the failure stress decreased with increasing die temperatures from 100 to 130 °C. The relaxation time had no correlation with the initial porosity because the relaxation time only affected the pellet quality at the end of the pellet production. As a result, the model could not predict a trend with respect to the relaxation time, but only with respect to the die temperature. The Panelli–Filhho model demonstrated a good fit with R^2 values ranging from 0.90 to 0.97. However, poor fits were observed when fitted with the relaxation time with R^2 values ranging from 0.78 to 0.79. Thus, the Panelli–Filhho model was only applicable to determine the relative density of compact at different temperatures. Generally speaking, the outcomes of the model fittings suggested that all the models, except Panelli–Filho Model, are capable of predicting pressure–volume relationship, yield strength, and plastic deformation behavior of Douglas fir pellets.

4.3. Mechanical test and energy usage

Table 5 lists the mechanical properties of Douglas fir pellets at different pelletization conditions. Asymptotic modulus is an indicator of the degree of stress relaxation of the pellets under a constant strain [8]. The lower the asymptotic modulus of the pellet, the higher the dimensional stability of the pellet. It was found that the asymptotic modulus was independent of the die temperature, but was highly affected by the applied pressure from 63 to 190 MPa. This concurred with the reduction of pellet density after a week's storage decreased to a minimum with increasing applied pressure from 63 to 126 MPa (Table 2). However, the reduction of

Table 5
Mechanical properties of Douglas fir pellets made at different pelletization conditions.

Die temperature (°C)	Pressure (MPa)	Relaxation time (s)	Asymptotic modulus (GPa)		Maximum breaking strength (MPa)	
			Average	SD	Average	SD
70	63	5	0.45	0.00	1.50	0.35
		15	0.43	0.01	1.39	0.36
		30	0.43	0.01	1.84	0.51
	126	5	0.89	0.01	2.75	0.94
		15	0.88	0.01	3.44	0.97
		30	0.85	0.02	2.60	0.26
	190	5	1.22	0.04	3.00	1.29
		15	1.19	0.01	3.16	0.67
		30	1.15	0.06	3.49	0.77
100	63	5	0.45	0.03	3.14	0.71
		15	0.46	0.03	3.53	1.58
		30	0.44	0.01	4.08	0.27
	126	5	0.91	0.04	5.37	1.32
		15	0.90	0.01	5.30	0.95
		30	0.86	0.02	4.75	1.28
	190	5	1.23	0.03	5.33	1.34
		15	1.17	0.00	5.38	1.95
		30	1.13	0.02	6.43	0.65
130	63	5	0.47	0.01	1.47	0.28
		15	0.45	0.01	1.47	0.26
		30	0.43	0.01	1.28	0.17
	126	5	0.94	0.03	2.08	0.36
		15	0.92	0.01	2.69	0.68
		30	0.89	0.03	1.96	0.46
	190	5	1.26	0.03	2.42	0.51
		15	1.20	0.04	2.98	0.58
		30	1.18	0.07	3.71	1.08

pellet density after a week's storage increased again when further compressed at a higher pressure of 190 MPa. This indicated that an excess applied pressure introduced an uneven stress distribution within the Douglas fir pellet and the residual stress built within the pellet became more difficult to relax. As a result, the resultant pellet was not dimensionally stable. This suggests that it is crucial to optimize the applied pressure of the pelletization to produce the most durable Douglas fir pellets.

From the hardness test, the maximum breaking strength of the Douglas fir pellets increased by four fold when the die temperature increased from 70 to 100 °C. During this temperature range, the water moisture (i.e. free water) vaporized and diffused into the middle lamella of the fibers to activate the lignin to undergo plasticization. Note that the glass transition temperature of the lignin is lowered with increasing moisture content from 8% to 10% of wood [33]. This facilitated the deformation of fibers to achieve optimum packing under compression. Therefore, the pellets made at 100 °C die temperature were found with the highest range of the maximum breaking strength between 3.53 and 6.43 MPa. However, the moisture was evaporated from the Douglas fir particles and lost to the atmosphere at a die temperature of 130 °C. This could not facilitate the plasticization of the lignin and the resultant pellet was found to have a decrease of maximum breaking strength. The resultant wood pellets were more likely to form dust upon external impact and subsequently causing dust explosion during transportation [34,35]. Therefore, Douglas fir pellets should not be produced at die temperatures higher than 100 °C. Since the term "durability" refers to describing how much fines will be produced from the pellets upon impact at the maximum fracture point, the maximum breaking strength obtained from the hardness test can be a good indicator to deduce the durability of Douglas fir pellets. Generally speaking, the die temperature is the most significant factor of determining the durability of the Douglas fir pellet followed by the effect of applied pressure.

Fig. 2 illustrates the energy consumption of pelletization at different applied pressures and die temperatures. The mid-point refers to the required energy input to produce pellets at a die temperature of 100 °C. The lower and higher end of the error bar shows the required energy input to produce pellets at die temperatures of 70 and 130 °C, respectively. The compression energy increased from 19.6 to 53.6 J/g with increasing applied pressure at the die temperature of 100 °C. The compression energy was found to be independent of the die temperature and relaxation time, but highly dependent on applied pressure. Extrusion energy did not occupy a significant portion of the total compression energy consumption [1] and therefore this study did not include an estimation of extrusion energy.

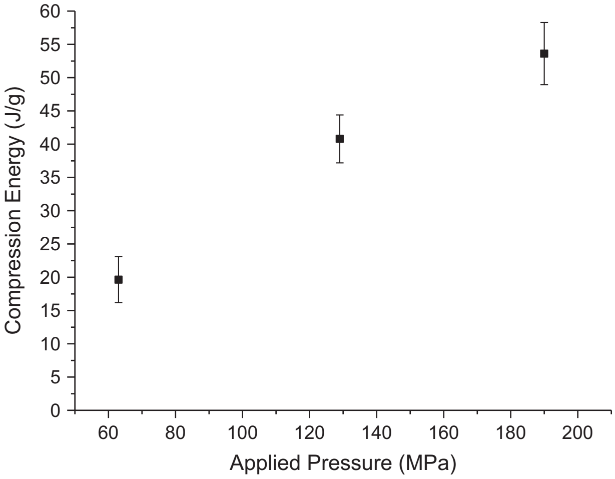

Fig. 2. Compression energy versus applied pressure with respect to different die temperatures of 70, 100 and 130 °C (*N* = 45).

5. Conclusions

The optimum processing condition to produce the best quality of Douglas fir pellets was 100 °C die temperature, 126 MPa applied pressure and 30 s relaxation time. The die temperature was recommended to operate below 100 °C to prevent moisture evaporation from particles. Temperature and applied pressure were governed in making denser pellets at temperatures lower and higher than 100 °C, respectively. All rheological models except the Panelli–Filho model were well described with respect to the compression behavior of Douglas fir ground particles. Compression energy was not affected by the temperature and the relaxation time, but only by the applied pressure.

Acknowledgements

This research is funded in parts by the Natural Sciences and Engineering Research Council of Canada (NSERC-CRD Grant: CRDPJ342219-06); Wood Pellet Association of Canada (Grant-11R42500). We acknowledge the support from Office of Biomass Program of the US Department of Energy.

References

[1] Lam PS, Sokhansanj S, Bi X, Lim CJ, Melin S. Energy input and quality of pellets made from steam exploded Douglas fir (*Pseudotsuga menziesii*). Energy Fuels 2011;25(4):1521–8.

[2] Lam PS. Steam explosion of biomass to produce wood pellets. Chemical & Biological Engineering, Vancouver, University of British Columbia. PhD Thesis; 2011.

[3] Sikanen L, Vilppo T. Small scale pilot combustion experiments with wood pellets – the effect of pellet length. Open Renew Energy J 2012;5:1–6.

[4] Kuokkanen M, Vilppo T, Kuokkanen T, Stoor T, Niinimäki J. Additives in wood pellet production – a pilot-scale study of binding agent usage. Bioresource 2011;6(4):4331–55.

[5] CEN/TC 335. EN 15210-1:2009 Solid biofuels – determination of mechanical durability of pellets and briquettes. Part 1: Pellets London; 2009.

[6] Shang L, Nielsen NPK, Dahl J, Stelte W, Ahrenfeldt J, Holm JK, et al. Quality effects caused by torrefaction of pellets made from Scots pine. Fuel Process Technol 2012;101:23–8.

[7] Lam PS, Sokhansanj S, Bi X, Lim CJ. Colorimetry applied to steam treated biomass and pellets made from western Douglas fir (Pseudotsuga menziesti L.). Trans ASABE 2012;55(2):673–8.

[8] Lam PS, Lam PY, Sokhansanj S, Bi XT, Lim CJ. Mechanical and compositional characteristics of steam-treated Douglas fir (*Pseudotsuga menziesii* L.) during pelletization. Biomass Bioenergy 2013;56:116–26.

[9] Tooyserkani Z, Kumar L, Sokhansanj S, Saddler J, Bi XT, Lim CJ, et al. SO_2-catalyzed steam pretreatment enhances the strength and stability of wood pellets. Bioresour Technol 2013;130:59–68.

[10] Adapa PK, Tabil LG, Schoenau GJ, Crerar B, Sokhansanj S. Compression characteristics of fractionated Alfalfa grinds. Powder Handl Process 2002;14(4):252–9.

[11] Denny PJ. Compaction equations: a comparison of the Heckel and Kawakita equations. Powder Technol 2002;127:162–72.

[12] Mani S, Tabil LG, Sokhansanj S. An overview of compaction of biomass grinds: powder handling and processing. Int J Stor Handl Process Powder 2003;15(3):160–8.

[13] Shaw MD, Karunakaran C, Tabil LG. Physicochemical characteristics of densified untreated and steam exploded poplar wood and wheat straw grinds. Biosyst Eng 2009;103:198–207.

[14] Jones WD. Fundamental principles of powder metallurgy. London: Edward Arnold Publishers Ltd.; 1960. p. 242–370.

[15] Heckel RW. Analysis of powder compaction phenomenon. Trans Metall Soc AIME 1961;221:1001–8.

[16] Cooper AR, Eaton LE. Compaction behavior of several ceramic powders. J Am Ceram Soc 1962;45(3):97–101.

[17] Kawakita K, Ludde KH. Some considerations on powder compression equations. Powder Technol 1971;4:61–8.

[18] Panelli R, Filho FA. A study of a new phenomenological compacting equation. Powder Technol 2001;114:255–61.

[19] Mani S, Tabil LG, Sokhansanj S. Evaluation of compaction equations applied to four biomass species. Can Biosyst Eng 2004;46(3):55–61.

[20] Tabil LG, Sokhansanj S. Process conditions affecting the physical quality of alfalfa pellets. Appl Eng Agric 1996;12(3):345–50.

[21] Stewart A. Pelleting of granular materials. Engineering 1938;169(4386):175–6. 203–204.

[22] Comoglu T. An overview of compaction equations. J Fac Pharm Ankara Uni 2007;36(2):123–33.

[23] ASABE Standards. S319.3: Method of determining and expressing fineness of feed materials by sieving, St. Joseph, Mich: ASABE; 2003.

[24] Krycer I, Pope DG, Hersey JA. The interpretation of powder compaction data – a critical review. Drug Dev Ind Pharm 1982;8(3):307–42.

[25] Moreyra R, Peleg M. Compressive deformation patterns of selected food powders. J Food Sci 1980;45:864–8.

[26] Scoville E, Peleg M. Evaluation of the effects of liquid bridges on the bulk properties of model powders. J Food Sci 1981;46(1):174–7.

[27] ASABE Standards. S358.2: Moisture measurement-forages. St. Joseph, Mich: ASABE; 2010.

[28] Sluiter A, Hames B, Ruiz R, Scarlata C, Sluiter J, Templeton D, et al. Determination of ash in biomass. NREL/TP-510-42622; NREL; 2008.

[29] Walker EE. The properties of powders-Part VI: the compressibility of powders. Trans Faraday Soc 1923;19:73–82.

[30] Chevanan N, Womac AR, Bitra VSP, Igathinathane C, Yang YT, Miu PI, et al. Bulk density and compaction behavior of knife mill chopped switchgrass, wheat straw, and corn stover. Bioresour Technol 2010;101:207–14.

[31] York P, Pilpel N. The tensile strength and compression behavior of lactose, four fatty acids and their mixture in relation to tableting. J Pharm Pharmacol 1973;25:1–11.

[32] Stelte W, Holm JK, Sanadi AR, Barsberg S, Ahrenfeldt J, Henriksen UB. A study of bonding and failure mechanisms in fuel pellets from different biomass resources. Biomass Bioenergy 2011;35:910–8.

[33] Goring DAI. Thermal softening of lignin, hemicellulose and cellulose. Pulp Pap Mag Can 1963;64:517–27.

[34] Calle S, Klaba L, Thomas D, Perrin L, Dufaud O. Influence of the size distribution and concentration on wood dust explosion: experiments and reaction modelling. Powder Technol 2005;157:144–8.

[35] Melin S. Testing of explosibility and flammability of airborne dust from wood pellets. Wood Pellet Association of Canada; 2008.